

FOREST BIODIVERSITY UNDER GLOBAL CHANGE

# Climate Change Effects on Vegetation Distribution and Carbon Budget in the United States

Dominique Bachelet,<sup>1\*</sup> Ronald P. Neilson,<sup>2</sup> James M. Lenihan,<sup>3</sup> and Raymond J. Drapek<sup>4</sup>

<sup>1</sup>Department of Bioresource Engineering, Oregon State University, Corvallis, Oregon 97331, USA; <sup>2</sup>USDA Forest Service, Forestry Sciences Laboratory, Corvallis, Oregon 97331, USA; <sup>3</sup>Department of Botany and Plant Pathology, Oregon State University, Corvallis, Oregon 97331, USA; and <sup>4</sup>Department of Forest Science, Oregon State University, Corvallis, Oregon 97331, USA

## ABSTRACT

The Kyoto protocol has focused the attention of the public and policymakers on the earth's carbon (C) budget. Previous estimates of the impacts of vegetation change have been limited to equilibrium "snapshots" that could not capture nonlinear or threshold effects along the trajectory of change. New models have been designed to complement equilibrium models and simulate vegetation succession through time while estimating variability in the C budget and responses to episodic events such as drought and fire. In addition, a plethora of future climate scenarios has been used to produce a bewildering variety of simulated ecological responses. Our objectives were to use an equilibrium model (Mapped Atmosphere–Plant–Soil system, or MAPSS) and a dynamic model (MC1) to (a) simulate changes in potential equilibrium vegetation distribution under historical conditions and across a wide gradient of future temperature changes to look for consistencies and trends among the many future scenarios, (b) simulate time-dependent changes in vegetation distribution and its associated C pools to illustrate the possible trajectories of vegetation change near the high and low ends of the tem-

perature gradient, and (c) analyze the extent of the US area supporting a negative C balance. Both models agree that a moderate increase in temperature produces an increase in vegetation density and carbon sequestration across most of the US with small changes in vegetation types. Large increases in temperature cause losses of C with large shifts in vegetation types. In the western states, particularly southern California, precipitation and thus vegetation density increase and forests expand under all but the hottest scenarios. In the eastern US, particularly the Southeast, forests expand under the more moderate scenarios but decline under more severe climate scenarios, with catastrophic fires potentially causing rapid vegetation conversions from forest to savanna. Both models show that there is a potential for either positive or negative feedbacks to the atmosphere depending on the level of warming in the climate change scenarios.

**Key words:** global climate change; simulation model; biogeography; carbon budget; MAPSS; MC1.

## INTRODUCTION

The Kyoto protocol agreement of December 1997 has focused the attention of the public and policy-

makers on the earth's carbon (C) budget. It has fostered a continuing search for a more accurate quantification of global terrestrial C sources and sinks to mitigate global climate change by conserving or increasing C sequestration. To estimate the size of C pools and fluxes, scientists have used biogeochemical models that simulate steady-state conditions using long-term average climatic records, or

Received 12 May 2000; accepted 22 November 2000.

\*Current address: Forestry Sciences Laboratory, 3625 93rd Avenue, Olympia, Washington 98512-9193, USA; e-mail: bachelet@fsl.orst.edu

temporal dynamics and interannual variability using annual climatic records. However, the climate can influence the C budget not only directly by affecting the flux rates but also indirectly by affecting both the disturbance regime and the vegetation type. Earlier research on climate change focused on changes in vegetation types and their C pools under doubled atmospheric carbon dioxide (CO<sub>2</sub>) concentration and associated climatic changes (VEMAP 1995). MAPSS (Mapped Atmosphere–Plant–Soil System), a biogeography model, has been used in this context to simulate vegetation distribution under several equilibrium climate change scenarios (VEMAP 1995; Neilson and others 1998; Neilson and Drapak 1998). The resulting vegetation maps have then been used by biogeochemistry models to determine the carbon budget estimates.

The equilibrium models require only long-term average climate and use biogeographic rules based on that climate to determine the vegetation type and its density. So the questions that remained were: How did this vegetation type come to be? Has it been a smooth transition from one vegetation type to another, or have there been abrupt changes and many transition states? Has there been a linear decline or an increase in biomass? To complement the “equilibrium snapshots” provided by the static models and answer these questions, new models have been designed to use transient climate and simulate dynamic changes in the vegetation type and its associated biogeochemical cycle. MC1 (Daly and others 2000) is one example of the new dynamic global vegetation models (DGVM) that can now illustrate year-to-year variability in the C budget due to climatic variations such as drought and disturbances such as fire under more realistic climate change scenarios that include the influence of dynamic oceans and aerosol forcing.

The existence of a large number of future climate change scenarios suggests that there is considerable uncertainty about possible future ecological impacts, particularly since some scenarios produce opposite sign ecological responses. However, Neilson and Drapak (1998) have discerned some patterns among six equilibrium scenarios and developed the hypothesis that moderate warming could produce increased vegetation growth over broad areas in the conterminous United States but greater warming could also produce large areas of drought stress and C losses.

In this paper, we further tested this hypothesis by providing a bridge between the sensitivity analysis of a static model (MAPSS) under many equilibrium scenarios and a time series analysis of a dynamic model (MC1) using only two of these scenarios but

treating them as transient scenarios—one with only a small amount of warming and one with a large amount of warming across the United States. MAPSS was run under seven equilibrium climate change scenarios at 10-km resolution. MC1 was run under two transient scenarios at 0.5° latitude/longitude resolution (approximately 50-km). The reason for the discrepancy between the number and the spatial resolution of the two types of scenarios is that (a) there are fewer transient climate change scenarios than equilibrium scenarios and (b) there are no transient climate change scenarios at 10-km resolution for the conterminous United States. To complete the bridge between equilibrium and transient analyses, we had to first show that the two models were reasonably consistent with each other in their responses under the various scenarios. The MAPSS and MC1 models are quite different in their structure and conception, so we did not expect perfect consistency. However, the broad patterns of future changes, particularly with respect to the sign and the location of the changes, had to be generally consistent. Therefore, MAPSS was also run at 0.5° resolution for the same two transient scenarios after they were averaged and transformed into equilibrium scenarios, and the results were compared to those of MC1.

Our objectives were thus to use both the static model MAPSS and the dynamic model MC1 to simulate (a) vegetation distribution (both models), (b) associated LAI (leaf area index—that is, area of leaves per unit area of ground, MAPSS) or biomass (MC1) and the interannual variations of the C fluxes (MC1), and (c) the resulting change in the extent and location of the stress areas (defined as areas of vegetation density reduction) in the conterminous US under historical conditions and under various climate change scenarios. Both models simulate vegetation changes using biogeographic rules based on climatic indices. Both simulate vegetation density. The equilibrium model works much more simply, using just LAI, which is a surrogate for vegetation density (high LAI for closed canopy, low LAI for low vegetation density), whereas the dynamic model simulates vegetation and soil C pools and fluxes. We focused our analysis on the conterminous United States, in part, because it may constitute a large C sink (Fan and others 1998) and also because we relied on the climate and soils datasets of the Vegetation/Ecosystem Modeling and Analysis Project (VEMAP), which are currently the highest quality datasets available (Kittel and others 1995).

The summaries of C gains or losses for the entire US can mask dramatic regional impacts. In our

study, simulated vegetation density in virtually all locations across the conterminous United States either increased or decreased under future climate scenarios. Even when the national average indicates an overall C gain under conservative climate change scenarios, regional droughts and fires can still cause significant distress to local ecological and economic systems. The rate of increase in forest vegetation density is constrained by its growth rate, which can lag behind climate change. On the other hand, the rate of decline in vegetation density is physically constrained by the rate of climate change and by episodic disturbance, and it can occur rapidly, even in forests. Simulated changes in either LAI or biomass were calculated to provide some indication of regional stress due to either drought or cold temperatures and some indication of regional gains due to moderate warming and increased precipitation. The location and extent of these regional stress areas is reported here because they should become the focus of the attention of land managers interested in sustainability issues.

## METHODS

### Models

Although there are many future climate change scenarios for equilibrium conditions that span a wide temperature increase gradient, there are still few transient scenarios available. Therefore, we used the MAPSS equilibrium model to illustrate potential vegetation responses to the variety of equilibrium climate change scenarios, and we also used MCI under two transient climate scenarios corresponding to the extremes of the temperature range of the equilibrium scenarios to illustrate the possible trajectories of vegetation types and C pools.

The MAPSS model (Neilson 1995) is an equilibrium biogeography model that includes a mechanistic hydrology module that calculates plant available water and a set of biogeography rules that determine climatic zone, life form, and plant type as a function of temperature thresholds and water availability (<http://www.fs.fed.us/pnw/corvallis/mdr/mapss>). MAPSS determines the maximum potential LAI a site can support, based on 1 year of long-term monthly average climate data, assuming the vegetation can use all available soil water. It simulates a CO<sub>2</sub>-induced increase in water use efficiency by reducing stomatal conductance by 35% at double the present CO<sub>2</sub> concentration (Eamus 1991). MAPSS uses an aerodynamic evapotranspiration approach that is sensitive to canopy characteristics. Grasses and trees have different rooting

depths in a three-layer soil and compete for available soil water, while shading by trees limits grass growth. Vegetation classification in MAPSS is based on climatic thresholds and the presence/absence and LAI values of three life forms—trees, shrubs, and grasses—with differing leaf characteristics, thermal affinities, and seasonal phenology. Either trees or shrubs are assumed to be dominant and mutually exclusive. There are 52 possible vegetation classes, but we aggregated them into 11 to simplify the visualization of the results in this paper (Table 1). MAPSS also includes a fire module that maintains prairie grasslands and transition zones such as the prairie peninsula. MAPSS cannot directly convert areas of decline in vegetation density to specific predictions of the amount of C lost because the simulations are based on leaf area, not C pool size.

MCI (<http://www.fsl.orst.edu/dgvm>) is the first version of a dynamic global vegetation model based on the linkage of MAPSS (Neilson 1995) and CENTURY (Parton and others 1987). The model (Daly and others 2000) reads monthly climate time series and calls first a set of biogeography rules that determines the vegetation type. Secondly, the model calls a modified version of the CENTURY model, where parameters vary as a function of the life form combination defined by the biogeography rules for that year. Once the C budget has been established and the soil moisture estimated, a fire module is called to determine if fuel load and fuel moisture are conducive to fire. Given adequate climatic conditions, a fire is simulated and C pools modified consequently. If the fire is extreme, the vegetation type may then be modified; for example, a burnt forest can become a grassland or a savanna.

MCI simulates mixtures of deciduous/evergreen and needleleaf/broadleaf trees and C3/C4 grass life forms using climatic thresholds modified from the original MAPSS biogeography rules. MCI classifies woody and herbaceous life forms into 24 different vegetation classes based on their leaf biomass simulated by a biogeochemistry module. The 24 classes were aggregated to 11 classes to simplify the visualization of the results in this paper (Table 1). The biogeochemistry module, a modified version of the CENTURY model, simulates plant production, soil organic matter decomposition, and water and nutrient cycling. It includes competition between trees and grasses for light, nutrients, and water. Production increases and transpiration decreases by 25% as atmospheric CO<sub>2</sub> concentration increases to 700 ppm. The hydrology module is a simple bucket model that, unlike MAPSS, does not include unsaturated flow. Potential evapotranspiration is calcu-

**Table 1.** Vegetation Classes: Comparison between MAPSS, VEMAP, and the Simplified Classification Used in this Paper

Simplified Classes (this Paper)	VEMAP Classes <sup>a</sup>	MAPSS Classes
1. Tundra	1. Tundra	601. Tundra
2. Taiga–Tundra	22. Taiga	600. Taiga–Tundra
3. Conifer Forest	2. Boreal Coniferous Forest	107. Forest EN Taiga
	3. Maritime Temperate Coniferous Forest	108. Forest Mixed warm EN
	4. Continental Temperate Coniferous Forest	112. Forest EN Maritime
	23. Boreal Larch Forest <sup>a</sup>	113. Forest EN Continental
4. NE Mixed Forest	5. Cool Temperate Mixed Forest	102. Forest Mixed Cool
5. Temperate Deciduous Forest	7. Temperate Deciduous Forest	100. Forest Deciduous Broadleaf
		111. Forest Hardwood cool
6. SE Mixed Forest	6. Warm Temperate—Subtropical Mixed Forest	101. Forest Mixed Warm DEB
7. Tropical Broadleaf Forest	8. Tropical Deciduous Forest	105. Forest EB Tropical
	9. Tropical Evergreen Forest	
8. Savannas and Woodlands	11. Temperate Coniferous Xeromorphic Woodland	109. Forest Seasonal Tropical ED
	13. Temperate Subtropical Savanna	110. Forest Savanna Dry Tropical ED
	15. Temperate Coniferous Savanna	200. Tree Savanna DB
	16. Tropical Deciduous Savanna	201. Tree Savanna Mixed Warm DEB
		205. Tree Savanna Mixed Cool EN
		206. Tree Savanna Mixed Warm EN
		207. Tree Savanna EN Maritime
		208. Tree Savanna EN Continental
		209. Tree Savanna PJ Continental
		210. Tree Savanna PJ Maritime
		211. Tree Savanna PJ Xeric Continental
9. Shrubs and Woodlands	10. Temperate Mixed Xeromorphic Woodland	301. Open Shrubland—No Grass
	12. Tropical Thorn Woodland	302. Shrub Savanna DB
	14. Warm Temperate Subtropical Mixed Savanna	303. Shrub Savanna Mixed Warm DEB
	19. Mediterranean Shrubland	307. Shrub Savanna Mixed cool EN
	20. Temperate Arid Shrubland	308. Shrub Savanna EN
		310. Shrub Savanna Subtropical Mixed
		311. Shrubland Subtropical Xeromorphic
		312. Shrubland Subtropical Mediterranean
		313. Shrubland Temperate Conifer
		314. Shrubland Temperate Xeromorphic Conifer
		423. Grass Semi Desert C3
		424. Grass Semi Desert C3-C4
10. Grasslands	17. C3 Grasslands	414. Grass Tall C3
	18. C4 Grasslands	415. Grass Mid C3
		416. Grass Short C3
		417. Grass Tall C3 C4
		418. Grass Mid C3 C4
		419. Grass Short C3 C4
		420. Grass Tall C4
		421. Grass Mid C4
		422. Grass Short C4
11. Arid Lands	21. Subtropical Arid Shrubland	305. Shrub Savanna Tropical EB
		309. Shrub Savanna Mixed Warm EN
		404. Grass Semi Desert
		425. Grass Semi Desert C4
		500. Desert Boreal
		501. Desert Temperate
		502. Desert Subtropical
		503. Desert Tropical
		504. Desert Extreme

E, evergreen; N, needleleaf; D, deciduous; B, broadleaf

<sup>a</sup>MCI simulates two categories beyond the 21 VEMAP classes: 22. Taiga and 23. Boreal Larch Forests.

lated using Linacre's (1977) equations. Nitrogen demand is always met in the current version of the model. Parameterization of the biogeochemical processes is based on the life form composition, which is updated annually by the biogeography module. The model also simulates the occurrence, behavior, and effects of severe wild fires (Lenihan and others 1998). Allometric equations are used to convert aboveground live and dead biomass to fuel classes. Fuel loading and fuel moisture thresholds are used to determine fire occurrence. Plant mortality, fire emissions, and live and dead biomass consumption are estimated as functions of fire spread, fire line intensity, and vegetation structure. Fire effects feed back to the biogeochemistry module to adjust the levels of the C and nutrient pools.

Because MCI is a carbon accounting model, vegetation and soil carbon pools need to be initialized. Soil C pools require a long time to build up. Consequently, the model is run on long-term mean climate (1 year of average monthly climate data) until the slow soil C pool equilibrates. This may require up to 3000 simulation years, depending on the ecosystem being simulated (Daly and others 2000). Because dynamic fire events cannot be simulated meaningfully using a mean climate, fire events are scheduled at regular intervals that vary with vegetation type. Once the soil C has equilibrated, the model is run on variable climate (spin-up period) allowing for fuel buildup and variable fuel moisture conditions until the aboveground C pools are at equilibrium with dynamic fire events. The spin-up climate timeseries is based on historical climate. Since the historical records contain known trends in both temperature and precipitation, they were detrended using a 30-year filter (VEMAP Members unpublished). After detrending, the long-term temperature and precipitation monthly averages were set equal to those of the first 15 years of the observed record (1895–1909) to provide a smooth transition into the observed records in 1895.

### Climate Scenarios

Seven future climate scenarios generated by general circulation models (GCM) were used by MAPSS at 10-km resolution (Kittel and others 1995; Neilson and Drapek 1998), and two of them were used by MCI and MAPSS at a  $0.5^\circ$  latitude/longitude resolution. Fine-scale features of the climate, related to topographic effects, are better represented in the higher-resolution (10-km) data set, and the large number of equilibrium scenarios provides a greater context to assess possible future changes. However,

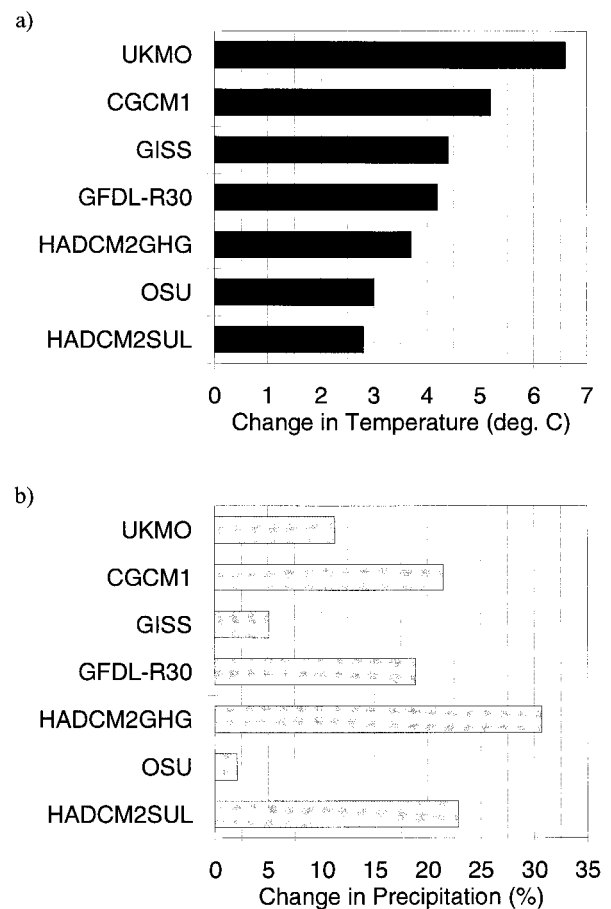


Figure 1. GCM-simulated changes in (a) temperature and (b) precipitation between historical and future conditions (at or near doubled  $\text{CO}_2$  values), aggregated over the conterminous United States. Transient model data were averaged for 1961–90 and 2061–99 and the difference are reported here. Transient GCMs include HADCM2SUL, HADCM2GHG (Johns and others 1997), and CGCM1 (Boer and others 1999). Equilibrium ( $2\times\text{CO}_2$ ) GCMs include OSU (Schlesinger and Zhao 1989), (Johns and others 1997), GFDL-R30 (Manabe and Wetherland 1990), GISS (Hansen and others 1988), and UKMO (Wilson and Mitchell 1987).

there are currently no 10-km transient climate data sets.

The scenarios span a range of about  $2.8$ – $6.6^\circ\text{C}$  in projected average annual temperature increase over the conterminous United States near the end of the 21st century (Figure 1). Four are equilibrium scenarios (GFDL-R30, GISS, UKMO, OSU) that were included in the First Assessment Report of the Intergovernmental Panel on Climate Change (IPCC) (Cubasch and Cess 1990). They include a single-layered ocean and assume an instantaneous doubling of  $\text{CO}_2$ . Three scenarios are transient and

were included in the Second Assessment Report of the IPCC (Gates and others 1996). Two transient scenarios come from the Hadley Climate Center (HADCM2GHG and HADCM2SUL, the latter of which includes effects of sulfate aerosols), and one comes from the Canadian Climate Centre (CGCM1, also including aerosols). Transient GCM include a fully dynamic 3-D ocean and are run from the 1800s to the present using observed CO<sub>2</sub> increases and into the future using IPCC projections of future greenhouse gas concentrations (IS92a) (Kattenberg and others 1995). The last 30 years of the three transient scenarios were averaged so they could be treated as equilibrium scenarios by the biogeography model, MAPSS. However, the transient scenarios were clearly not at equilibrium, having attained only about half to two-thirds of their eventual temperature change, due to thermal inertia of the oceans (Gates and others 1996). Only HADCM2SUL and CGCM1 were used to run MCI. The 0.5° latitude/longitude transient climate data set was generated in the context of the VEMAP, aggregating some of the 10-km data, such as precipitation. The baseline historical climate corresponds to VEMAP Phase 1 baseline climate.

### Calculation of Stress Area

Using both models (MAPSS and MCI), we simulated the fractional area of US land that underwent a decline in vegetation density (where vegetation density was less than its long-term mean) under all scenarios (seven for MAPSS, two for MCI) and termed this the “stress area index,” or SAI. Using MCI, we followed the temporal trajectory of the SAI through the past 100 years and into the future to the end of the 21st century. Because MAPSS simulates LAI rather than biomass, we used changes in LAI as an approximation of changes in vegetation density and compared them with changes in biomass calculated by MCI. Even though LAI and biomass are curvilinearly related, changes in both should follow the same direction and occur in the same geographic regions.

In most cases, the cause of stress is drought that follows either a reduction in precipitation, an increase in evaporative demand (higher temperatures), or both. Our analysis is similar to the spatial mapping of the Palmer drought severity index (PDSI) (Palmer 1965). The objective is to relate regional patterns of drought or vegetation stress to large-scale atmospheric circulation changes on both short and long time scales (see for example, Nigam and others 1999), because the SAI essentially tracks the regional wet and dry zones partitioned by persistent jet stream positions.

*MAPSS simulations at 10-km resolution.* For each grid cell, we calculated the difference between the average LAI under a future climate change scenario (between 2070 to 2099 for the three originally transient scenarios) and the average LAI for the historical period from 1961 to 1990. The fraction of the US lands and forested areas where that difference was negative ( $LAI_{2070-2099} < LAI_{1961-1990}$ ) was defined as the SAI.

*MCI simulations at 0.5° latitude/longitude.* We first calculated the long-term average live vegetation carbon simulated for the spin-up climate time series (detrended historical climate) described earlier. We then calculated, for each year of the simulation and for each grid cell, the difference between the current year’s simulated live vegetation C and that from the spin-up period. The fraction of the US lands and forested areas where that difference was negative (live vegetation carbon<sub>year</sub> < live vegetation carbon<sub>spin-up average</sub>) was defined as the SAI.

## RESULTS AND DISCUSSION

### Potential Vegetation Distribution

*MAPSS Results under seven GCM scenarios (10-km resolution).* Over 40% of the coniferous forests are replaced by savannas under the UKMO scenario (Figures 2 and 3). Under all other scenarios (except GISS), coniferous forests expand slightly (Figure 2). The temperate deciduous forest shifts to more northern locations (Figure 3) and is replaced by either the southeast mixed forest or savannas under most scenarios except for the mildest one (HADCM2SUL). Northeast mixed forests are replaced by either savannas (UKMO, GFDL) or the northward-shifting temperate deciduous forest. Southeast mixed forest are replaced mostly by savannas under three scenarios: the UKMO scenario and CGCM1, which project the largest increases in temperature (both above 5°C), and the GFDL scenario. Southeast mixed forest are even replaced partially by grasslands under the two warmer scenarios (Figure 3). Tropical forests appear as a new vegetation type mostly in Louisiana (Figure 3), where they replace the original Southeast mixed forest. The area covered by all forest types tends to decrease by the end of the 21st century under the warmest scenarios (over 40% under the UKMO scenario, about 20% for CGCM1 and the GFDL scenario) (Figure 4a). In contrast, moderately warm scenarios (HADCM2SUL and HADCM2GHG) produce increases in forest area of about 20%.

MAPSS simulates decreases in shrubland area under all scenarios except the UKMO scenario and HADCM2SUL, where shrubs replace grasses in ar-

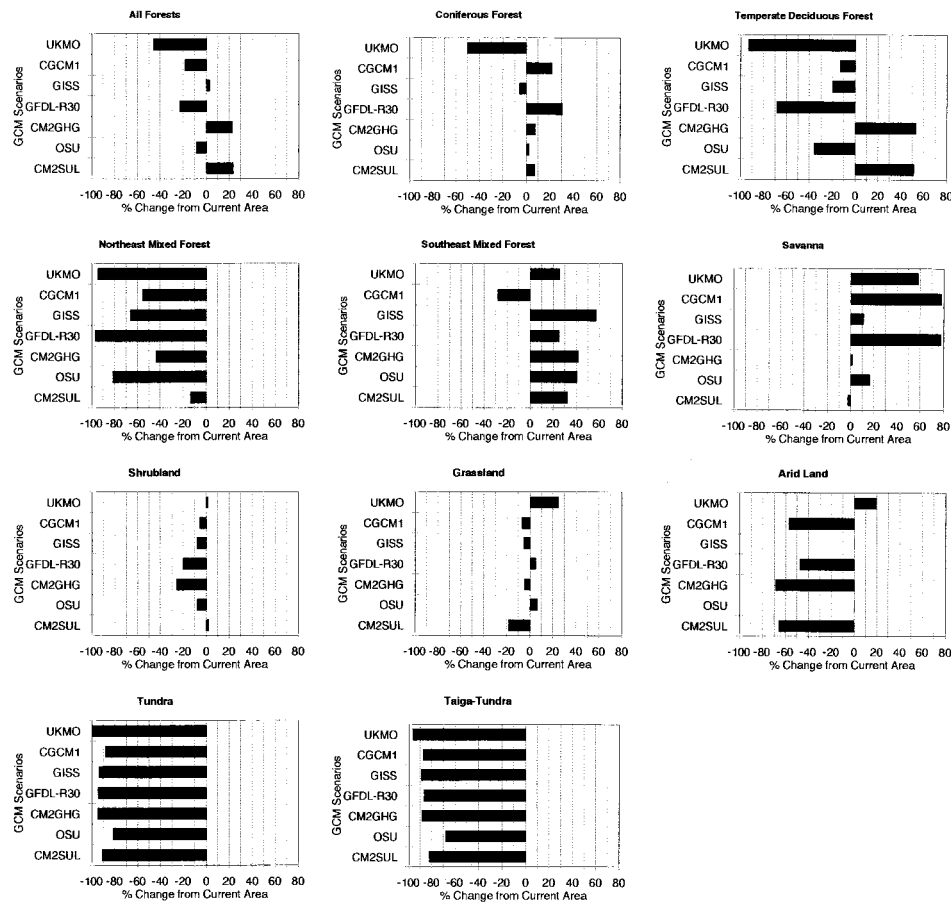


Figure 2. Percentage change in area (10-km resolution) of 11 simplified vegetation types for the conterminous US between current and future conditions under the seven GCM scenarios listed in Figure 1.

eas of the Great Plains (Figure 3). Most shrubland losses occur in the Great Basin, where increased precipitation drives the replacement of shrubs by savannas. Savannas are simulated to increase by more than 50% under three warm scenarios (UKMO, CGCM1, GFDL) (Figure 2). The area occupied by grasslands is relatively stable (Figure 2), except for a 20% increase in area simulated under the UKMO scenario, where they expand into Minnesota and Wisconsin, and a 20% decrease under HADCM2SUL, where they are replaced mostly by savannas (Figure 3). Simulations for the western United States show 60% or greater reductions in the area of deserts under HADCM2SUL, HADCM2GHG, and CGCM1 (Figure 2). MAPSS simulates about a 50% decrease in the area of arid land under the GFDL scenario, but with only small changes to the extent of the Sonoran Desert (Figure 3). MAPSS simulates a 20% increase in desert area only under the warmest scenario, UKMO (Figure 2).

MAPSS simulates some of the largest percentage changes at high elevations where taiga-tundra and

tundra decrease by more than 80% by the end of the 21st century (Figure 2).

*MAPSS and MC1 results under two transient scenarios (0.5° latitude/longitude resolution).* Under historical climate, MC1 simulates that over 40% of the US is covered by grasslands, whereas MAPSS simulates that only about 25% of the US is covered by grasslands (Figure 5a). MAPSS simulates about 15% of the US being covered by shrubs and woodlands, whereas MC1 simulates only about 1% of the US covered by shrubs and woodlands.

In general, the two models agree with each other on both the sign and magnitude of the simulated future changes. Both models agree that the largest percentage change is the disappearance of the taiga-tundra and tundra vegetation types from the continental US due to increases in temperature (Figure 5). Both models simulate decreases in the area of arid lands, due to increased precipitation and simulated increased water-use efficiency under elevated atmospheric CO<sub>2</sub> (Figures 5 and 6). Both models agree that grassland area decreases and that shrub and woodland areas increase under both fu-

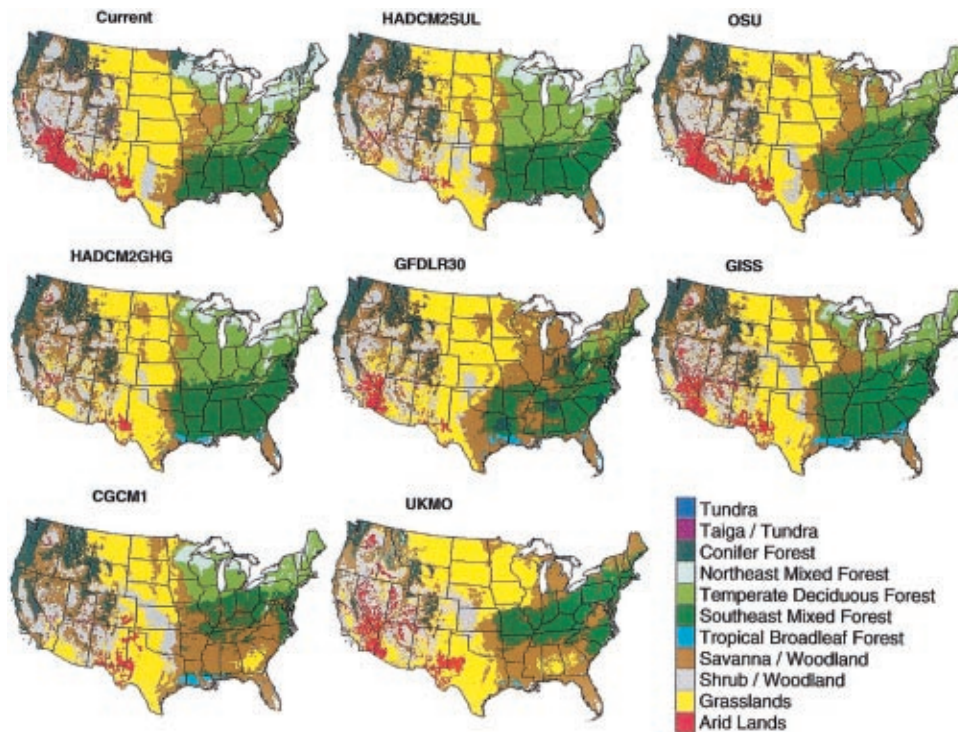


Figure 3. MAPSS-simulated vegetation distribution for the conterminous US (10-km resolution) under the seven GCM climate scenarios listed in Figure 1.

ture climate change scenarios (Figure 5). However, MAPSS simulates a 75% increase in savanna area under CGCM1, whereas MC1 simulates a 30% decrease. Under HADCM2SUL, both models simulate little change in savannas and woodlands (small decreases with MCI, small increases with MAPSS). Both models predict an encroachment of tropical forests along the Gulf Coast in the Southeast under both scenarios.

Both models predict small decreases in the area of temperate deciduous forests under CGCM1 and small increases under HADCM2SUL (Figure 5). The two models show losses of northeast mixed forests under CGCM1, large for MAPSS (approximately 90%), moderate for MC1 (approximately 20%). However, the two models disagree on the fate of northeast mixed forests under HADCM2SUL: significant losses for MAPSS (approximately 65%) and moderate gains for MC1 (about approximately 30%), especially in Minnesota and Wisconsin, where they replace savannas and grasslands. The two models also disagree on the sign of the response of coniferous forests.

*Comparison between the two models.* At coarse resolution, MAPSS simulates a smaller extent of historical grasslands and shrublands and a larger extent of shrublands and woodlands than MC1 in greater agreement with Küchler's (1975) map of potential vegetation (Figure 5a). This large difference between the two models is due in part to the

dynamic fire model in MC1. The grassland areas that are classified as shrub and woodlands by MAPSS are areas of high fire-return intervals. MC1 biogeography rules may underestimate the contribution of the shrubs to the landscape using temporal averages of total leaf biomass because of the recurring loss of shrub leaf biomass in fires. On the other hand, MAPSS does not include a dynamic fire module; thus, it may miss the secondary effect of droughts, fueling fire events, and it may overestimate vegetation density. This difference between the two models is carried into simulations of the future. In these simulations, MAPSS always simulates more shrubs and woodlands than MC1, and MC1 simulates more grasslands than MAPSS (Figure 6).

MAPSS and MC1 simulate similar changes in future vegetation distribution. However, they disagree about the extent of savanna area primarily because of the simulated response of the southeast mixed forests. With MAPSS, savannas replace much of the southeast forests; with MC1, the Southeast remains dominated by forests even though their density is lower than that of the original southeast mixed forests (Figure 6). The two models also disagree on the sign of the response of coniferous forests. Coniferous forests include both northeastern boreal coniferous forests and northwestern temperate coniferous forests. The boreal forests in the Northeast shift north and decrease in



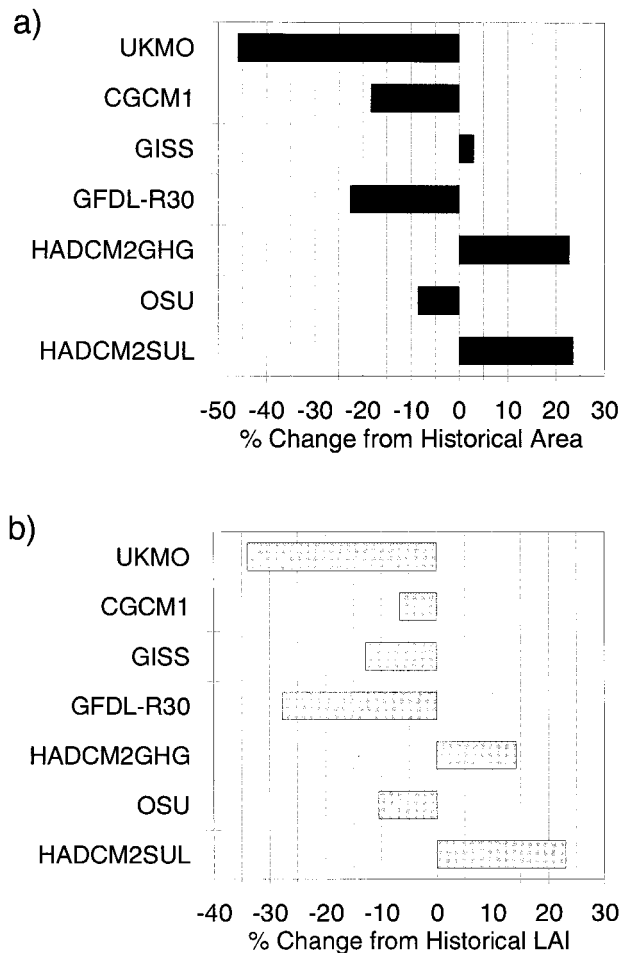


Figure 4. Percentage changes in (a) forest area and (b) forest LAI for the conterminous US between current and future conditions for the seven GCM climate scenarios listed in Figure 1.

area for both models and under both scenarios. Thus, the disagreement between the models is really about the fate of western coniferous forests. Western coniferous forests increase in area under both scenarios with MAPSS at the 10-km resolution and with MC1 at the 0.5° resolution, but they show little change under either scenario for MAPSS at the coarser resolution. Because the higher-resolution climate data set captures more accurately the complex topography of the western states, MAPSS results at the 10-km resolution should be more reliable.

It is more difficult to explain why MC1 simulations with coarse resolution climate do not agree with MAPSS results at the same resolution. It may be due to scaling of climate or different sensitivities of the models to subtle differences in climate. MAPSS is very sensitive to variations in vapor pres-

sure deficit (VPD), a variable not utilized by MC1. VPD was calculated and scaled differently between the two different resolutions of climate data (Neilson 1995; VEMAP 1995) and may be causing the different responses. The large sensitivity of MAPSS to VPD arises from the aerodynamic evapotranspiration algorithm used in the model (Marks and others 1998). It has been shown that different algorithms produce different sensitivities to climate change (Mckeeney and Rosenberg 1993). However, a full analysis of the MAPSS VPD sensitivity would require a complete replacement of the evapotranspiration algorithm and a recalibration of the model; it is therefore beyond the scope of this paper.

The different responses of the Northeast mixed forests between MAPSS and MC1 result from uncertainties regarding the relative importance of water and/or temperature in controlling the competitive relationship between temperate deciduous and Northeast mixed forests. Under both scenarios, there are subregions in the northeastern region of the US that become wetter and other subregions that become drier. Under both scenarios, temperatures get warmer. Thus, the limiting factors of temperature and drought play complex roles in both models in this region and different nuances in implementing these two factors produce different responses.

*Comparison of MAPSS results across scales.* Disagreement in the sign of change between fine and coarse resolution MAPSS results (Figure 5c, d) occurs for shrubs and woodlands and for western coniferous forests. Because these vegetation types are typically found in western states, we believe the higher resolution climate, which more accurately simulates small climatic variations due to the complex topography, enables the model to better simulate the vegetation response to climate changes. We have thus relied primarily on the 10 km results for past assessment work. In the case of savannas under the HADCM2SUL scenario, the magnitude of the simulated change is small under both scenarios, and the disagreement in the sign of change between the two resolutions is probably due to a simple accounting of the pixels involved, —a resolution error rather than a disagreement in the prediction.

There are differences in the magnitude of change between fine- and coarse-resolution MAPSS results especially for the northeast mixed forests, which are replaced by temperate deciduous forests at the coarser resolution under HADCM2SUL (Figure 6d). As with the conifer response in the West, the difference between resolutions may be a result of differences in the VPD calculations.

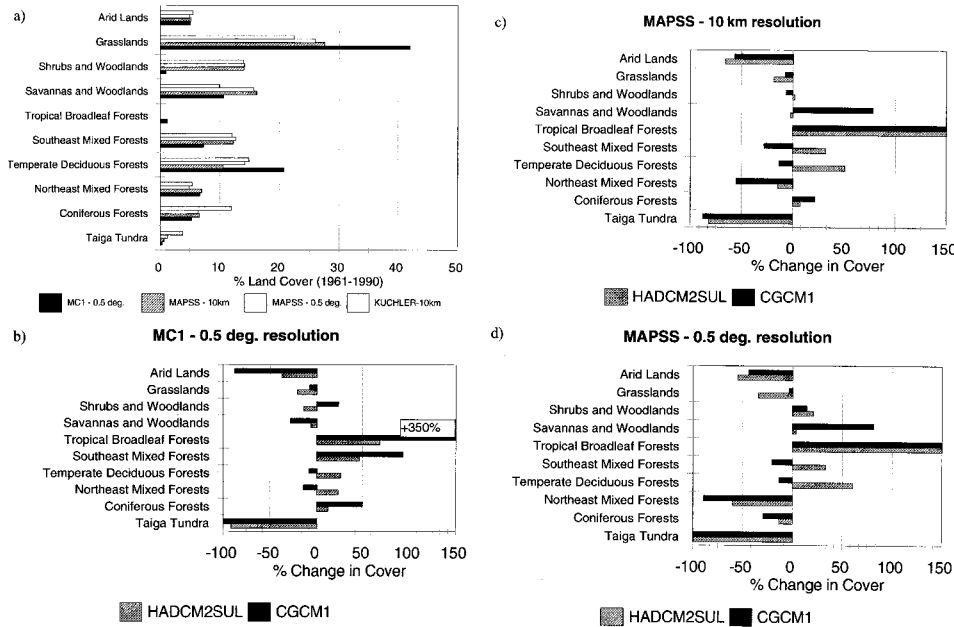


Figure 5. (a) Percentage land cover of simplified potential vegetation types simulated by MC1 (1990) and MAPSS (baseline historical climate) over the conterminous US compared to Kuchler's (1975) potential vegetation map. (b) Percentage change in area of the simplified vegetation types as simulated by MC1 under two transient scenarios for the year 2095. (c) Percentage change in area of the simplified vegetation types as simulated by MAPSS at 10-km resolution under an average climate (2070–99) from the same two scenarios (since there were no tropical broadleaf forests under historical conditions, percentage change has been arbitrarily set to 150%). (d) Same as c, but for 0.5° latitude/longitude resolution.

## LAI and Vegetation Biomass

*MAPSS-simulated LAI under seven CGM scenarios (10 km resolution).* MAPSS simulates large increases in LAI both in the Southwest (California, Arizona, and Nevada) and in the East (Figure 7) under both Hadley Climate Center scenarios, which simulate the greatest increases in precipitation (more than 22%) and also produce only modest warming. Under CGCM1, MAPSS also simulates large increases in LAI in the West but large decreases in LAI in the East. Under the OSU, GFDL, GISS, and UKMO scenarios, MAPSS simulates large decreases in LAI in the Great Lakes area, New England, and along the southern coast (Figure 7).

MAPSS consistently predicts increases in LAI for savannas, shrublands, and arid lands under all scenarios (Figure 8) with LAI increasing by nearly 500% in desert areas under CGCM1. The LAI of both southeast mixed forests and temperate deciduous forests increase by up to 70% under the wettest climate scenarios with modest warming (such as HADCM2SUL), but they decrease under the warmer climate scenarios. Large decreases in LAI are simulated for the Northeast mixed forest except under the more modest warming scenario, HADCM2SUL. Increases in LAI are simulated for the taiga–tundra area (up to +241%) except under the warmest scenario (UKMO), where the decrease

in LAI reaches almost 50%, and under the GFDL-R30 scenario (Figure 8). The overall trend for all the forest types combined is similar to that observed when looking at the change in area, with forest LAI increasing under wetter scenarios with modest warming and declining under the warmer scenarios (Figure 4).

*Change in LAI (MAPSS) and live vegetation carbon (MC1) under two transient scenarios (0.5° latitude/longitude resolution).* MAPSS and MC1 simulate lower vegetation density for coniferous forests under both transient climate change scenarios (Figure 9a). This decrease pertains only to those areas currently populated by conifers—that is, the Northeast and the Northwest. Drought-induced vegetation density reductions occur in parts of both regions, even though increased precipitation allows conifers to expand into northern California and the Great Basin. Both transient climate change scenarios produce precipitation increases in the southern half but some decreases in the northern half of the western US, thus causing some vegetation declines in those areas.

MC1 simulates an increase in vegetation density in the northeast mixed forest under HADCM2SUL, whereas MAPSS simulates no change. However, under CGCM1, both models simulate a decrease in vegetation density (Figure 9). Both models predict an increase in the LAI of temperate deciduous for-

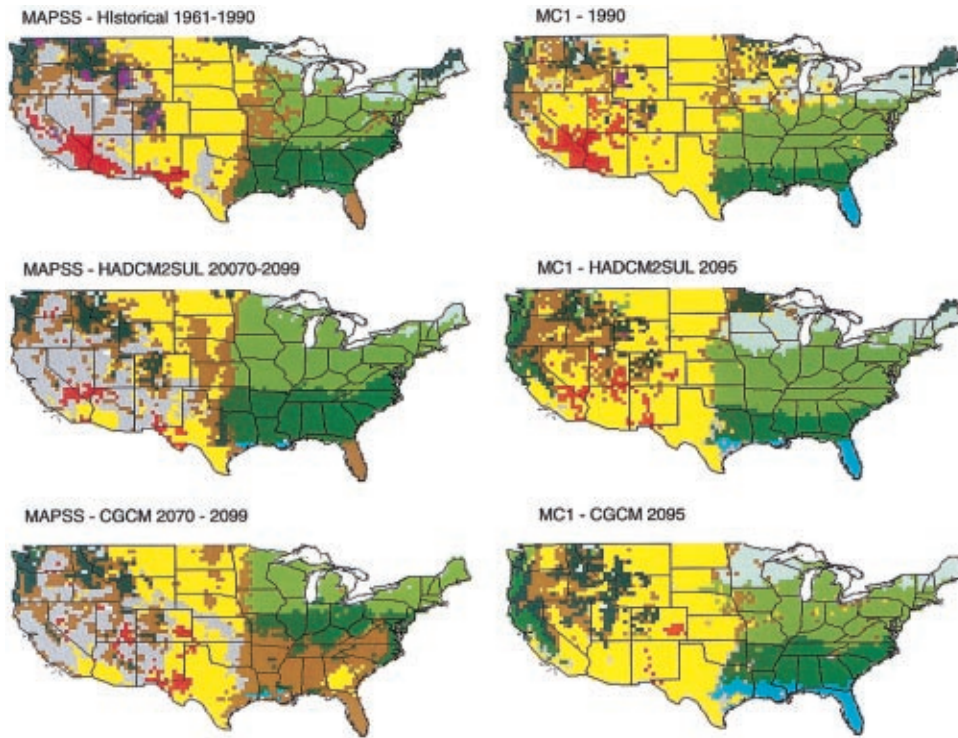


Figure 6. Potential vegetation distribution simulated by MAPSS and MC1 for current conditions (baseline historical climate for MAPSS, 1990 for MC1) and for future conditions (2070–99 for MAPSS and 2095 for MC1) under two scenarios: HADCM2SUL and CGCM1 at 0.5° latitude/longitude resolution. The color legend is identical to that of Figure 3.

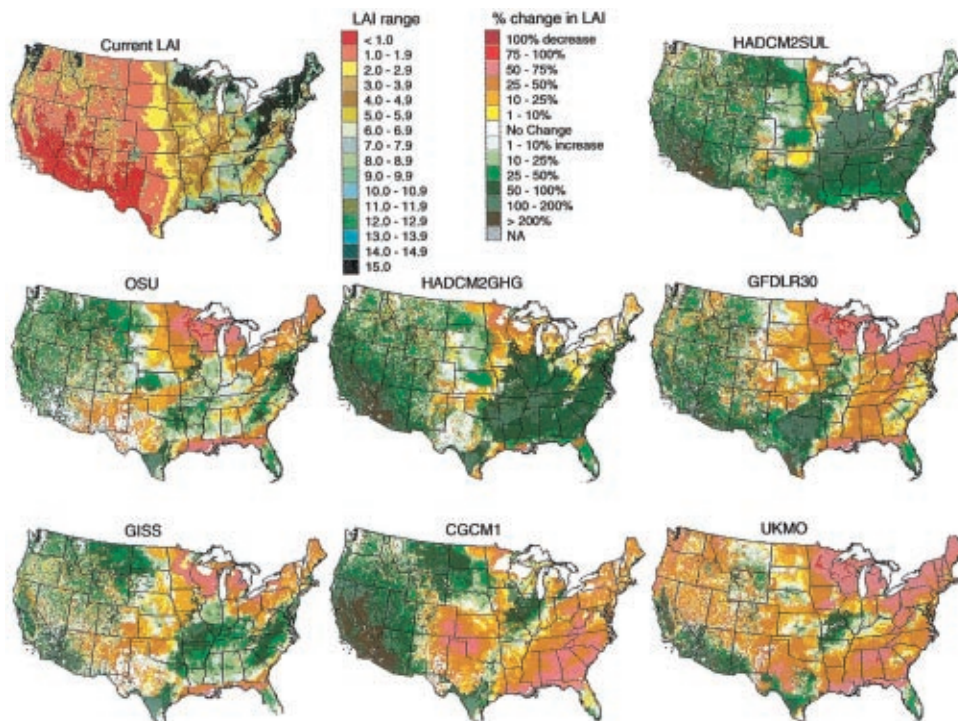


Figure 7. MAPSS-simulated LAI at 10-km resolution for current climate conditions and percentage change in LAI under the seven GCM climate scenarios listed in Figure 1.

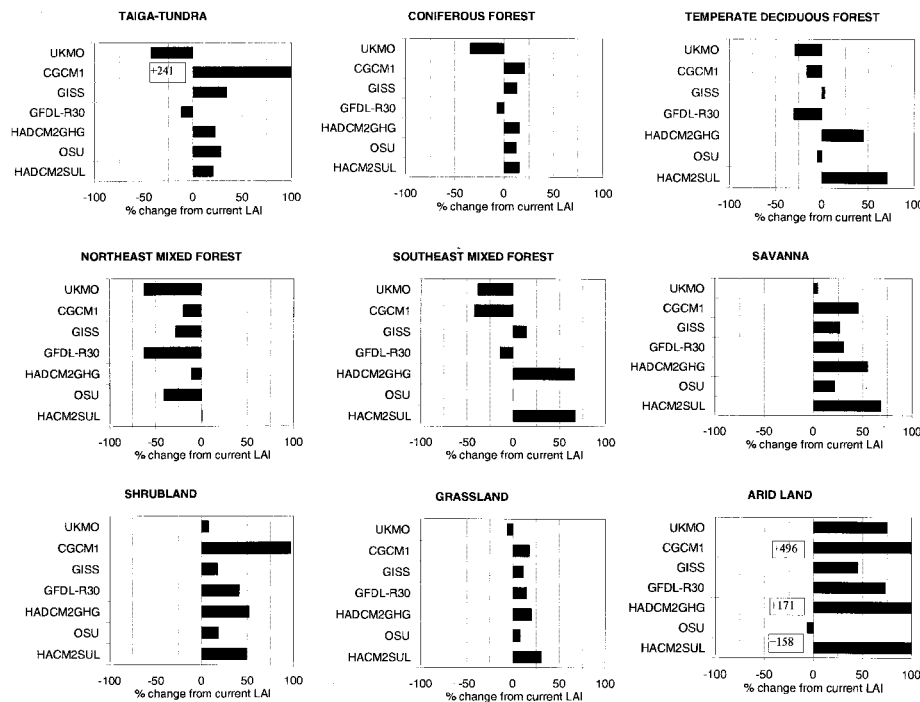


Figure 8. MAPSS-simulated percentage change in LAI at the 10-km resolution for each simplified vegetation type over the conterminous US between current and future conditions under the seven GCM scenarios listed in Figure 1.

ests under both scenarios. For southeast mixed forests, MC1 and MAPSS simulate an increase in vegetation density under HADCM2SUL and a decrease under CGCM1.

MC1 simulates a decrease in vegetation C in tropical broadleaf forests under both scenarios. MAPSS does not include tropical forests under historical climate conditions. Both models simulate increases in the vegetation density of savannas, shrublands, grasslands, and arid lands.

*Comparison of MAPSS results across scales.* Simulations by MAPSS of coniferous forests LAI (Figure 8) showed an increase under most climate change scenarios at 10 km resolution except under the more extreme UKMO scenario, whereas they showed a decrease at 0.5° latitude/longitude resolution (Figure 9). Coniferous forests correspond in our simple classification to a combination of northeastern boreal and western conifer forests. We showed earlier that they respond differently to climate change and that, because of the complex topography of the western US, western conifer forest simulations were sensitive to scaling. We have more confidence in the validity of high-resolution results because of the greater accuracy of the climate simulation at that scale.

MAPSS simulates an increase in the LAI of temperate deciduous forests under both transient scenarios at coarse resolution in contrast to the 10 km

resolution results under CGCM1 (Figures 8 and 9). The differences between the results from MAPSS at the two resolutions may be due to the VPD differences in the baseline climates, but in any case they highlight the sensitivity of western vegetation to subtle variations in climate.

*Temporal dynamics of net biological production (NBP) and carbon pools (MC1 simulation).* Total C storage remains stable (135 Pg C) in the early part of the 20th century until about 1940, when it begins to increase (Figure 10a). The upward trend beginning around 1940 corresponds to an increase in precipitation over North America and the beginning of three decades of Northern Hemisphere cooling (Karl 1998). This trend is also reflected in the net biological production (NBP) trace (Figure 10d). NBP, calculated as the net change in C storage from one year to the next and equivalent to net primary production NPP minus heterotrophic respiration and fire emissions, averages  $-0.6 \text{ Pg C y}^{-1}$  from 1895 to 1940, when a warmer climate with frequent droughts favors C fluxes from decomposition, respiration, and fire; by contrast, from 1940 to 1971, cool climate favors C sequestration and NBP averages  $+0.12 \text{ Pg C y}^{-1}$ .

Impacts of large fire events and droughts (particularly in the 1910s and 1930s) in the early part of the 20th century are clearly visible in the evolution of NBP. The same impacts are also probably respon-

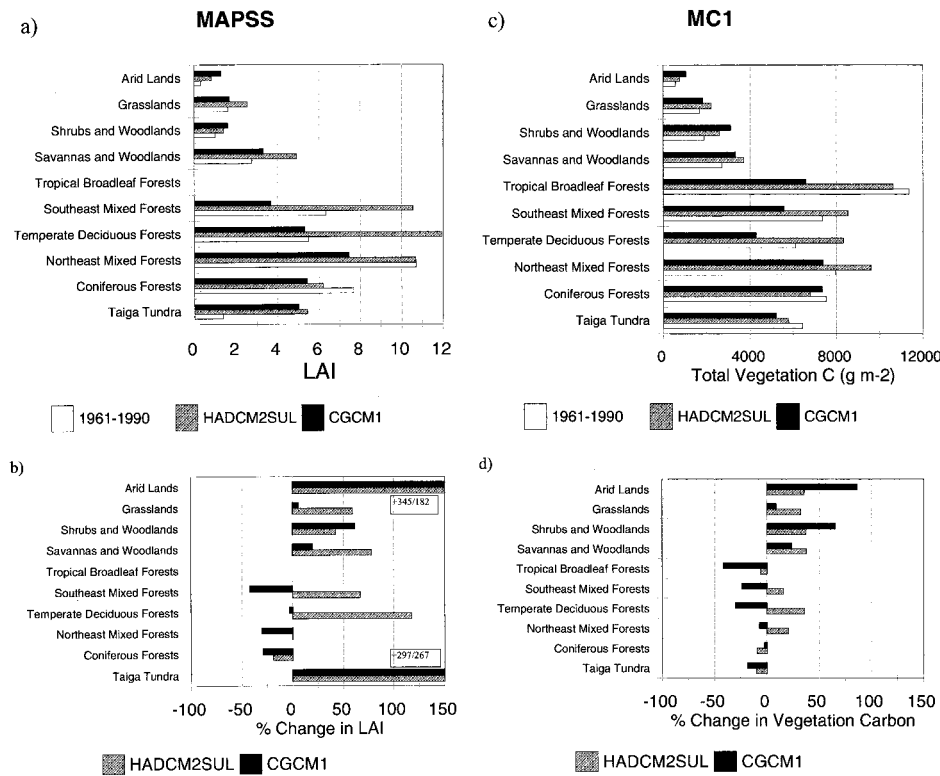


Figure 9. MAPSS-simulated LAI (a) and percentage change in LAI (b). MC1-simulated live vegetation carbon (c) and percentage change in vegetation carbon (d) for historical and future conditions under HADCM2SUL and CGCM1 at 0.5° latitude/longitude resolution for 11 simplified vegetation types. MAPSS results are for the average climate of 2070–99. MC1 results are averaged over the decade of the 2090s.

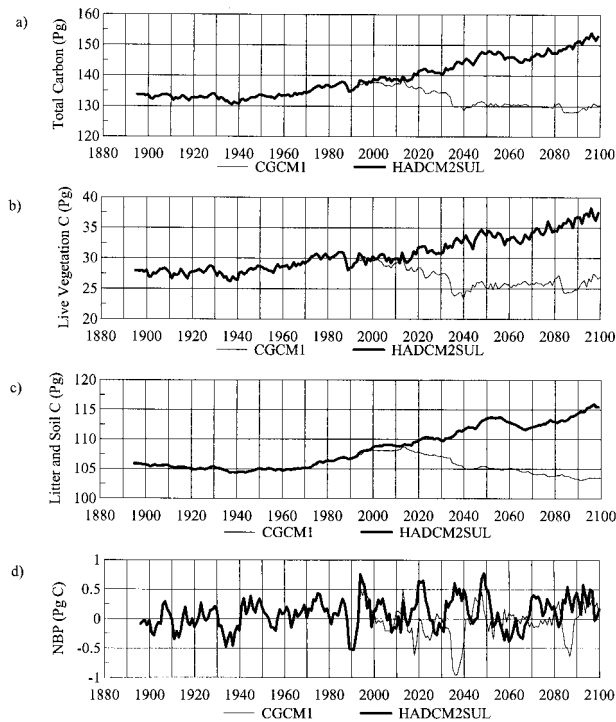


Figure 10. Temporal dynamics (simulated by MC1) of (a) total vegetation and soil C (b) live vegetation C (c) litter and soil C, and (d) net ecosystem productivity (NBP, defined as gain or loss in total C from one year to the next) under HADCM2SUL and CGCM1.

sible for the small decline in soil C during the same period (Figure 10c). Nicholls and others (1996) report that the Northern Hemisphere shifted from 3 decades of cooling to a persistent warming trend in 1972 or 1976, depending on the region, and was accompanied by a large increase in precipitation over North America (Karl 1998). Again, this regime switch is captured in the simulation of NBP, which decreases slightly to an average of +0.09 Pg C y<sup>-1</sup> between 1971 and 1993, when we can assume plant and soil respiration are again enhanced by warmer temperatures.

To further verify MC1 simulations, we compared NBP results with recently published values. MC1 simulated NBP averages +0.06 Pg C y<sup>-1</sup> between 1961 and 1990. Even though these NBP values include no history of land use, such as agricultural conversion and forest harvest, they agree well with simulations by other VEMAP models (0.08 Pg C y<sup>-1</sup>) that included agricultural ecosystems (Schimel and others 2000), but they are lower than the observed record for forests of about 0.3 Pg C y<sup>-1</sup> (Birdsey and Heath 1995; Houghton and others 1999). Regrowth of eastern US forests following harvest is thought to be responsible for the higher observed NBP (Schimel and others 2000) and the discrepancy between observations and simulations that do not include land-use history.

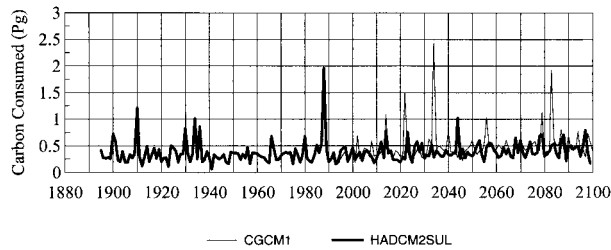


Figure 11. Simulated (MC1) total annual C consumed by wildfire for the conterminous US under HADCM2SUL and CGCM1. These results are potential dynamic vegetation only and do not include land-management activities, such as fire suppression, forest harvest, or conversion to agriculture.

*The role of fire in the carbon budget (MC1 simulation).* MC1 simulates an increase in the frequency of fires during the 1930's drought and a large fire event in 1988, a major fire year in the western United States (Sampson 1997), when the model simulated 2 Pg C  $y^{-1}$  consumed (under potential natural conditions—that is, without agriculture) (Figure 11). MC1 simulates that fires consumed about 720 Tg C  $y^{-1}$  between 1895 and 1993. This is consistent with Leenhouts's (1998) estimate of 530–1228 Tg C  $y^{-1}$  during the same period for potential natural vegetation in the conterminous United States.

Simulations of C pools by MC1 differ dramatically between the two transient scenarios. MC1 simulates a continuous increase in total biomass, litter, and soil organic C under HADCM2SUL (Figure 10a). However, under CGCM1, it simulates a 15% decline in total live biomass (Figure 10b) and a 5% decrease in litter and soil organic matter (Figure 10c) over the course of the 21st century. Biomass consumed by fire increases in the future under HADCM2SUL (Figure 11). Around 2044, fires consume about 1 Pg C, causing a sharp decline in biomass (Figure 10a, b). No single fire event seems correlated with the sharp decline in live vegetation from 2057 to 2067, although the large negative NBP during that period indicates a strong drought response (Figures 10c, d). Under CGCM1, total live biomass decreases while biomass consumed by fire increases, especially around 2030, when fires consumed almost 2.5 Pg C, largely in eastern forests (Figures 11 and 12). Around 2085, also under CGCM1, large fires correspond to large declines in total biomass (Figures 10a and 11). Fire increases in the West under both scenarios (Figures 12e, f), but especially under CGCM1, because fuel loads increase with increased precipitation coupled with several wet–dry cycles (El Niño/La Niña).

## Stress Area

*Linear relationship between stress area and temperature increase.* Across the seven climate change scenarios (10-km resolution), there is a significant relationship between the projected increase in temperature and the stress area simulated by MAPSS over the conterminous United States (Figure 13). MAPSS simulates an 11% increase in this area per degree of temperature increase (Figure 13a). Considering only the forest lands, the stress area simulated by MAPSS increases at a rate of 17% of the total forest area per degree of increased temperature (Figure 13b). The stress area simulated by MC1 (0.5° latitude/longitude resolution) at the end of the 21st century compares well with that simulated by MAPSS (Figure 13) for both conterminous US lands and forested areas under both scenarios. Under HADCM2SUL, at the low end of the temperature gradient represented by the seven scenarios, MC1 simulates an area of vegetation stress of about 20% of the conterminous US, whereas MAPSS simulates 10%. Under CGCM1, MC1 simulates almost 60% and MAPSS almost 40% of the total area undergoing some stress (Figure 13a). However, both models show greater sensitivity of forests under the warmer scenario with MC1 simulating nearly 80% and MAPSS about 55% of current forest area losing carbon under drought stress by the end of the 21st century (Figure 13b). The MC1 results under the two scenarios lie within the range of variation of the MAPSS results under all seven scenarios. Both models also show that forest areas are more sensitive than non-forest areas to potential future temperature increases. The overall response of both models across a range of scenarios suggests that an average annual temperature increase of 4.5°C could produce a reduction in vegetation density over about 50% of conterminous US forest lands, while the remaining lands would experience increased growth. This temperature increase corresponds to about the middle of the projected temperature change over the conterminous US by the end of the 21st century.

### *Time Series of Historical Stress Area Compared to the Drought-Area Index (MC1 Simulation)*

The stress area simulated by MC1 varies considerably from year to year. Large droughts clearly stand out. The drought of the 1930s is simulated as the most severe of the century, affecting about 49% of the simulated forest area and about 60% of the US land surface between 1933 and 1940 (Figure 14). These results agree with a time series of a drought-area index (DAI) based on the PDSI (Palmer 1965). The DAI is the area of land with a PDSI value

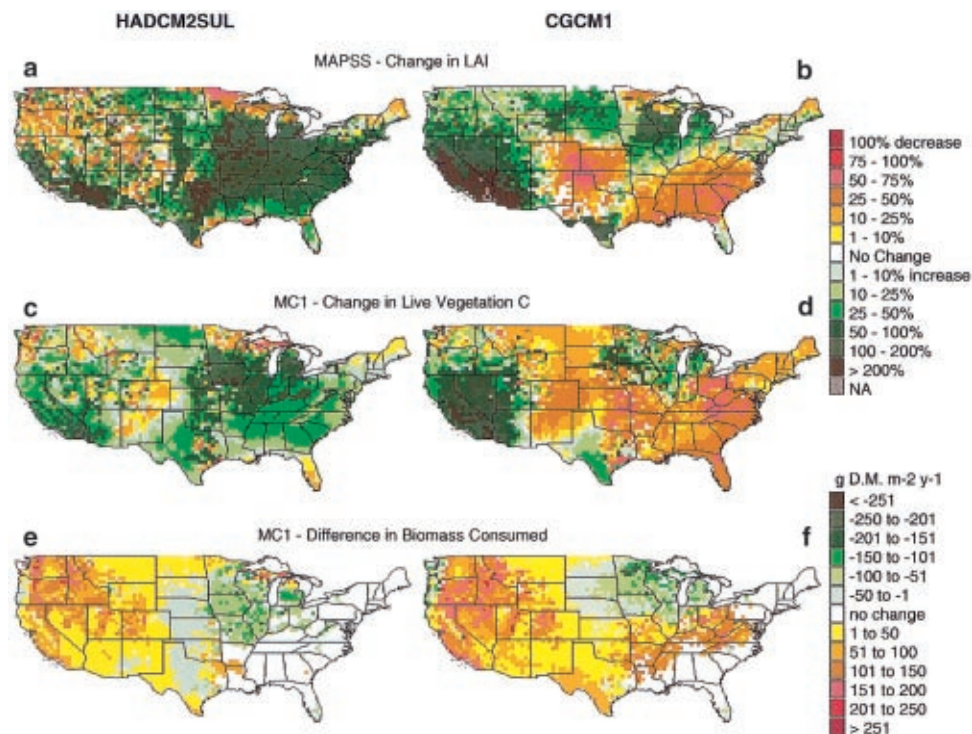


Figure 12. (a), (b) Simulated percentage change in LAI (MAPSS model at  $0.5^\circ$  latitude/longitude resolution) vs (c, d) change in live vegetation carbon (MC1) under HADCM2SUL and CGCM1 scenarios. MAPSS results are the change between the 2070–99 period and the baseline historical period. MC1 results compare average vegetation carbon of the last decade of the century to that of the 1961–90 period. (e, f) Absolute change in average annual biomass consumed as simulated by MC1, comparing the long-term average for the entire historical period (1895–1993) to that of the entire future climate change period (1994–2099) under HADCM2SUL and CGCM1.

showing moderate to extreme drought (Diaz 1983). The DAI indicates that the three major drought episodes during the 1930s affected between 50% and 80% of the conterminous US (Diaz 1983). The drought of the 1950s (1951–57), as simulated by MC1, affects about 49% of the forest area and about 53% of the entire conterminous United States. Again, this result is confirmed by the DAI, which indicates that an area of 50% to more than 60% of the US was involved in that drought (Diaz 1983). Finally, as simulated by MC1, between 1988 and 1992, about 39% of the US was losing C under drought stress. This result agrees with Changnon's (1989) estimate (based on the PDSI) that about 40% of the US was under severe to extreme drought in 1988 alone. MC1 simulated that the brunt of the 1988 drought was in nonforested zones with only about 25% of the simulated forest area being affected by it.

**Evidence of the 1972 climatic shift.** The stress area simulated by MC1 averages 49% of the conterminous US during the historical period until about 1972, when it drops to 34% and remains at that level until 1993. The decline in the stress area in 1972 is particularly large across forest lands (Figure 14b), dropping from a pre-1972 average of 43% to a post-1972 average of about 27%. This result compares well with climatic observations. The rapid decline in stress area in 1972 can be linked to a

dramatic increase in the precipitation regime over North America and the shift from 3 decades of cooling to persistent warming (Karl 1998).

**Projection of the future extent of the stress area.** The stress area simulated by MC1 in the future is quite different under the two scenarios (Figure 14). Under HADCM2SUL, there is an initial increase followed by a continuous decline in the stress area, which implies that increased precipitation associated with moderate warming and coupled with  $\text{CO}_2$  effects is favoring vegetation growth (Figure 14a, b). Under CGCM1, the stress area increases in the early decades of the 21st century, returning to the level of the 1930s drought, and remains at that level until the end of the century (Figure 14a). The amount of forested stress area under CGCM1 shows the same pattern as that of the overall stress area, but it is far greater than during any of the drought episodes of the past century (Figure 14b), reaching nearly twice the average level of the past century (from a pre-1972 value of 43% to about 80% of current forest area).

## SYNTHESIS

### Changes in Vegetation Distribution

**Consistent patterns across all climate change scenarios.** Our first objective was to see if there were consistent patterns of vegetation change across a large

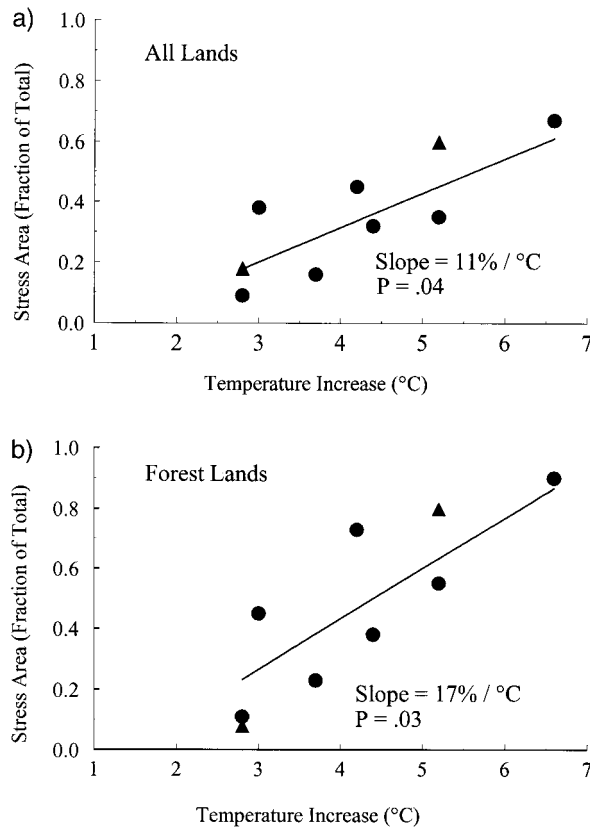


Figure 13. Fractional area of LAI decline (stress area) as a function of the average change in temperature over the conterminous US from the seven GCM scenarios listed in Figure 1, as simulated by MAPSS (●) for (a) the conterminous US land area and (b) the forested lands only within the conterminous US at 10-km resolution, including the least-squares regression line. For comparison, the stress areas simulated by MC1 (▲) are also shown for two transient scenarios (HADCM2SUL and CGCM1), representing the regions of live biomass decline, comparing the last decade of the 21st century to the historical period (1961–90) at 0.5° latitude/longitude resolution.

gradient of temperatures simulated by GCM using the equilibrium vegetation model, MAPSS. Many results are indeed consistent across all scenarios. For example, under most scenarios, MAPSS simulates increases in vegetation density in the southwestern states, where large increases in precipitation contribute to the reduction of arid land areas (Figure 3). MAPSS also simulates some vegetation decline in the Great Lakes region, particularly in the area of northeast mixed forests, subject to warmer and drier climatic conditions in the 21st century (Figure 3). Under most scenarios, MAPSS simulates decreases in the area of tundra and taiga–tundra that disappear as their cooler temperature optima

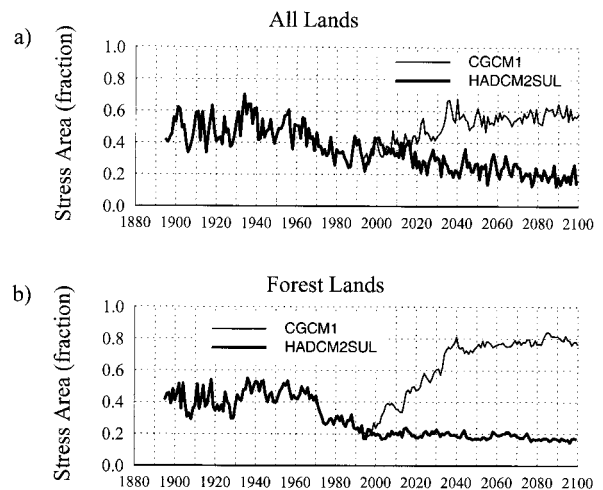


Figure 14. MC1-simulated stress area under historical climate and future climate scenarios for (a) the conterminous US and (b) forested lands only. The stress area is the area of the US or of the US forest lands where live vegetation C density is less than that of the long-term average carbon density calculated for the 100-year spin-up period.

disappear (Figure 2). On the other hand, MAPSS simulates increases in the area of southeast mixed forests and savannas under most scenarios (Figure 2).

There are also trends across the scenarios that seem related to the magnitude of the potential increase in future temperatures. MAPSS simulates an overall increase in vegetation density with moderate warming and a decrease with greater warming. Biomes that appear most sensitive to elevated temperatures include the temperate deciduous forest, which decreases in area under the warmer scenarios but increases under the more moderate scenarios, and the southeast mixed forest, which shifts northward under the warmer scenarios and is replaced by savannas and grasslands in its current location (Figure 2). Conifer forests show some indication of increased sensitivity with increasing temperature, but their overall response is less clear because they increase slightly in area under most but not all scenarios (Figure 2).

*“Early green-up, later browning” hypothesis.* MAPSS results across the seven climate change scenarios imply a monotonic change in climate: neither interannual nor interdecadal variability affect these equilibrium simulations. Were the climate to change in such a smooth manner and temperatures to increase to the level projected by the warmest scenario, simulation results suggest the possibility



for an early green-up in response to a moderate warming, followed later by vegetation density declines due to temperature-induced droughts (Neilson and Drapek 1998). We had hoped to test this hypothesis with a dynamic global vegetation model, such as MCI, using a climate change scenario from the warmer end of the temperature gradient, such as CGCM1. However, even though temperatures tend to increase somewhat monotonically in these scenarios, precipitation exhibits considerable interdecadal variability, which can override the simplified trajectory implied by the hypothesis. Although precipitation under CGCM1 increases significantly by the end of the 21st century, it first decreases by 4% by mid-century before increasing rapidly to the end of the century. Because temperatures increase in the first few decades of the 21st century as precipitation slightly decreases, the hypothesized early green-up does not materialize under CGCM1. Instead, there is a rapid loss in vegetation density until mid-century, after which increasing precipitation and water-use efficiency roughly balance the increasing evaporative demand (Figures 10 and 14). It is not clear what would have prevailed had CGCM1 continued with increased warming beyond the 21st century. A more thorough test of the early-greening, later-browning hypothesis would require the use of several transient climate change scenarios.

*Moderate warming benefits vegetation but additional warming could cause droughts.* In addition to testing the early-greening, later-browning hypothesis, we were interested in comparing the results from the two types of models and in integrating these results in an overall synthesis that would enhance our confidence in the conclusions. Although there are differences between MAPSS and MCI results, the similarities are striking. In general, both models agree that, under moderate warming, vegetation density increases due to the projected increase in precipitation and CO<sub>2</sub>-induced increases in water-use efficiency, resulting in forest expansion and C sequestration across the United States. They also agree that greater warming can lead to lower vegetation density and conversions of forests to savannas and grasslands with possible overall losses of C to the atmosphere in regions where neither precipitation increases nor direct CO<sub>2</sub> effects can compensate for the exponential increases in evaporative demand.

Regional projections illustrate this pattern. Both models agree that warming produces a northward shift of the various eastern forest types and an altitudinal shift of the colder taiga-tundra and tundra vegetation types, which may have disappeared by the end of the 21st century from the conterminous

United States (Figure 5). However, steep mountain slopes with unstable or poorly developed soils may limit the upslope migration of forests. The two models also agree on the contraction of the Southwest arid land area (Figure 5) associated with large increases in LAI or biomass in several southwestern states (California, Nevada, and Arizona), due to the predicted increases in precipitation (and CO<sub>2</sub>-induced water-use efficiency) accompanying the rise in temperature (Figure 12).

Both models simulate increases in the area of southeast forests (Figure 5) under HADCM2SUL and decreases in their vegetation density under CGCM1 (Figure 9). The C losses suggested by MAPSS are sufficient to convert much of the Southeast forests to savannas and grasslands, whereas losses simulated by MCI are considerable but not sufficient to cause a conversion to savanna. Simulated fires by MCI convert large sections of the Southeast to savannas and grasslands by the middle of the 21st century. However, these savannas recover to forests by the end of the 21st century, even though their biomass remains approximately 30% lower than before the fires,—not far in character from the savannas simulated by MAPSS. Areas in the Southeast that were near the fire zones, but not burned, also experience drought-induced vegetation density declines of about 30%.

The fate of the western coniferous forests under warmer climates is less clear. MCI simulates a large expansion of the coniferous forests across the western states under CGCM1, even though it simulates a decrease in their C density over the area of their current distribution. MAPSS, on the other hand, simulates little change in their area but a decrease of their LAI under the two transient scenarios at low resolution (0.5° latitude/longitude). However, MAPSS simulates an increase in the western coniferous forest area and in their LAI at higher resolution (10-km) under most scenarios (except UKMO). Because the higher-resolution climate takes into account complex terrain, it includes less scaling error and thus should produce more reliable simulations. It is important to note that both models assume that there are no barriers to species migration, such as seed dispersal limitations or habitat loss due to urban or agricultural expansion.

Under CGCM1, both models simulate decreases in biomass or LAI in the Great Plains states (Colorado, New Mexico, Texas, Oklahoma, Kansas). MCI also simulates large decreases in biomass in Arkansas, Missouri, Oklahoma, and Kansas and in the Carolinas, West Virginia, and Ohio with

conversions to savannas and grasslands under CGCM1 (Figure 12). In these eastern forest areas, MCI simulates increases in fire frequency. Because MAPSS does not include a dynamic fire module, it may miss the secondary effect of droughts, fueling fire events, and it may overestimate vegetation density.

Two regions where the two models disagree and where the scale of the input data affects simulation results stand out for their apparent sensitivity to climatic changes and should be the object of further research: (a) the Southeast, where the more severe climate change scenarios induce large declines in C stocks, and, (b) the northwestern forests, where complex topography and uncertainties about precipitation change and potential CO<sub>2</sub>-induced water-use efficiency render predictions more tentative.

### Carbon Budget under Future Climate Conditions

*A warming threshold separates the future green world from the brown world.* Under HADCM2SUL, MCI simulates a C gain of approximately about 15 Pg in the US terrestrial biosphere from now to the end of the 21st century, whereas under CGCM1, it simulates a loss of around 7 Pg C over the conterminous US (Figure 10). Even though neither positive nor negative feedbacks from the biosphere have been included in the climate change scenarios, feedbacks are implied in the simulation results because the conterminous US can become either a C source or a C sink depending on the scenario. These results suggest that there is a warming threshold transition point. Below this temperature threshold (for example, HADCM2SUL), plants could thrive and their C uptake could slow global warming (negative feedback). However, above this threshold (CGCM1), regional drought stress could occur and cause net C emissions (for instance, from drought and fires) that could accelerate global warming, producing additional vegetation stress (positive feedback). Past simulations suggest that these concepts apply globally, rather than simply to the US (Neilson and others 1998; Neilson and Marks 1994).

### Stress Area Trajectories

*Historical records confirm model projections of location and extent of stress areas.* The stress area trajectories (Figure 14) are analogous to the widely used approach of the Palmer drought severity index to track national changes in overall drought stress and to map the area over which drought impacts are

important. MCI tracks the drought area index (based on PDSI) quite well over the historical time frame, capturing the well-known droughts of the 1930s, 1950s, and late 1980s, among others. Thus, these results provide some measure of validation of the model. The stress area trajectories also hint of a climate regime shift about 1972, which corresponds to a large shift in both the temperature and rainfall regimes over North America at that time (Karl 1998). PDSI maps are often used to indicate large-scale atmospheric circulation regimes, their relationship to interdecadal oceanic circulation regimes, and their shifts to alternative states (Nigam and others 1999). The regime shift identified by Nigam and others (1999) occurred in 1976. Both years, 1972 and 1976, appear to be important atmospheric change points. A climate regime shift also occurred in 1940 (Neilson 1986), corresponding to a change from Northern Hemisphere warming to 3 decades of cooling and also to an increase in precipitation over North America (Nicholls and others 1996). All of these atmospheric circulation regime shifts are apparent in the evolution of NBP (Figure 10), shifting from a long-term negative annual average of  $-0.06 \text{ Pg C y}^{-1}$  to a positive average of  $+0.1 \text{ Pg C y}^{-1}$  after 1940. The climate shift in 1972 also produced a minor reduction in NBP from  $+0.12$  (1940–71) to  $+0.09 \text{ Pg C y}^{-1}$  (1972–1993).

*Under the canadian future climate change scenario, the largest stress area is in the southeast.* Future stress area trajectories are of interest when looking at the potential consequences of mild vs more extreme warming. The position of storm tracks or jet stream patterns influences the location of regions of increased moisture and of drought-stressed areas. Under HADCM2SUL, MCI simulates a continuous reduction in the drought-stressed area; under CGCM1, it simulates an overall increase in that area (Figure 14). The stress area under CGCM1 increases rapidly over the 3–4 decades, then stabilizes for the rest of the 21st century, suggesting a large regime shift in the atmospheric circulation. As temperatures increase during these first decades, CGCM1 precipitation decreases slightly during the same period. However, both temperature and precipitation increase during the latter period, but the area over which stress impacts occur appears to stabilize by mid-century. Most of the drought region is concentrated in the eastern to southeastern US, with a predominant impact on forests. These temporal and regional changes suggest a significant reorganization of the upper atmospheric circulation patterns. Which of these two scenarios, if either, is more

likely to occur cannot be stated at this time. More transient scenarios must be analyzed to see if there are any overall tendencies, or if there are uniquely different atmospheric circulation regimes that tend to occur under the different scenarios.

### Validation Efforts

Cramer and others (1999) and Scurlock and others (1999) have emphasized the need for improved validation methods to more accurately evaluate the sensitivity and validity of model responses to climatic signals. Cramer and others (2000) compared six DGVM under HADCM2SUL as they simulate vegetation changes and C fluxes for the globe. Like MC1, two of these DGVM are derived from equilibrium biogeography models—LPJ from BIOME3 (Sitch and others 2000), and SDGVM (Woodward and others 1998) from DOLY—and include both biogeography rules and mechanistic physiological and biogeochemical processes, but they also include a detailed calculation of photosynthesis. Three others—IBIS (Foley and others 1996), TRIFFID (P. Cox personal communication) and VECODE (Brovkin and others 1997)—also include feedback fluxes to the atmosphere because they were originally designed to be included in coupled atmosphere–biosphere models. MC1 does not include these biofeedbacks, which can greatly modify atmospheric responses to changes in albedo and evaporation fluxes, for example. Cramer and others (2000) compared their vegetation distribution results to a satellite-derived map of the world and their simulated fluxes with published estimates (for example, see Ciais and others 1995; Fung and others 1997). Because of the coarse spatial resolution of their results, the vegetation distribution maps are difficult to compare with those presented here. However, in terms of C fluxes, when MC1 was run with the same climatic data, it showed a much lower sensitivity to CO<sub>2</sub>, probably due to its lack of a detailed representation of photosynthesis (including a direct relationship to atmospheric CO<sub>2</sub> concentration), and projected a future global C source rather than a C sink for the 21st century. Future net ecosystem production (NEP) simulated by MC1 did not show the CO<sub>2</sub> fertilization effect compensating for the impacts of global warming. One of the DGVM—LPJ (Sitch and others 2000)—used in Cramer and others (2000), has also been run with the 0.5° latitude/longitude resolution climate data for VEMAP and has displayed a much stronger response to enhanced CO<sub>2</sub> than MC1, confirming the importance of adequate representation of CO<sub>2</sub> effects on plant processes, the lack of data about CO<sub>2</sub>

impacts at the regional scale during the 20th century, and the resulting inability of modelers to refute either projection. Clearly, more work needs to be done to create databases that can be used by modelers to verify their projections.

The simulation by MC1 of biomass consumed by fire over the historical period bears some relationship to the stress area calculations (Figures 11 and 14). Fires tend to occur in the heart of the drought zones, given sufficient fuel (Figure 12). However, the stress-area and biomass-consumed curves are not exact overlays, because most biomass consumed comes from forests and the historical droughts affected forested and nonforested regions differently. Even so, the fact that MC1 accurately captured known high-fire years, such as 1910 and 1988, provides another test of the validity of the model. Several other validation efforts are under way, comparing model results with extensive soil and vegetation databases available for the states of Oregon and Washington (M. Harmon, B. Law, S. Remillard personal communication), as well as other data sets gathered from the literature. Because the models do not simulate historical or future land use, it is difficult to directly compare the results of the simulations with field data. Land-use impacts, forest harvest patterns, and disturbances (for example, fire, pests, disease) need to be taken into account during the validation exercises. Efforts are currently under way to begin including land-use changes in simulations of historical vegetation dynamics and these changes also need to be considered in future scenarios. In addition, models can always be improved through reexamination and improvement of existing model processes.

### Conclusions and Options for the Future

We have attempted to bring some clarity to the confusion surrounding the multitude of possible future climates and the associated ecological responses. Rather than focusing on a single scenario, which may seem less confusing but is inherently deceptive, we have chosen to examine as many scenarios as possible to see if there were any consistent patterns. The use of the MAPSS equilibrium biogeography model allowed us to examine seven scenarios, but only as “snapshot” comparisons of current vs future conditions. That is, it provides no indication of how the biosphere might evolve dynamically between the current conditions and the end of the 21st century.

Consistent patterns have emerged from our comparison of the seven scenarios. In some instances,

all seven scenarios produced the same sign of change—for example, spatial shifts of cold-limited ecosystems. In other instances, certain trends followed the increase in temperature across all seven scenarios, where regional differences in precipitation produced the “noise” around the regression line; for example, forest area might increase under mild warming but decrease under greater warming. Similarly, the area of the US subjected to drought stress appeared to increase linearly with respect to the projected temperature change. A 4.5°C rise in temperature could cause drought stress in about 50% of US forest area (while the other 50% shows increased growth), suggesting that a temperature increase near 4.5°C could be a threshold below which US ecosystems would sequester C but above which they would lose C.

The MC1 results provided some sense of how the terrestrial biosphere could change along two trajectories chosen among the seven scenarios—one near the mild end of the temperature change gradient and one near the warm end. The overall results from MC1 were quite consistent with those from MAPSS, even though there were some differences in the details. As hypothesized from the MAPSS results, the moderately warm Hadley scenario (HADCM2SUL) produced increased vegetation growth and reduced drought stress throughout the 21st century. Also as anticipated, the warmer Canadian scenario, which exceeds the 4.5°C threshold, produced large areas of drought stress, resulting in net C losses by the end of the century. However, the Canadian scenario deviated from the “linear” logic of the MAPSS-based hypothesis of early green-up followed by later browning. The hypothesis presumed that precipitation increased linearly with temperature, which did not happen in the Canadian scenario because drought stress began almost immediately. These results should not be taken too literally, since a different Canadian simulation with different initial conditions might produce a different trajectory. Nevertheless, these results underscore the importance of interannual and interdecadal climate variability, the potentially large impact of climate variations on ecosystems, and the need for further use and development of dynamic vegetation models using various ensembles of climate change scenarios.

Finally, both transient scenarios included large changes in regional weather patterns. Each scenario, even the milder HADCM2SUL scenario, produced regional impacts of drought and fire

that could cause significant distress to regional ecological and economic systems, while warmer and wetter climates could benefit other regions.

Given the uncertainty surrounding future scenarios, managers would be well advised to develop contingency plans for alternative futures, increased vegetation growth, or increased vegetation stress, with specific regional patterns and timing to both. Monitoring could be configured to identify these alternative conditions as they occur. One of the greatest uncertainties in these results is the importance of the CO<sub>2</sub>-induced water-use efficiency, which is incorporated in all results presented here. If the effect is less than that simulated, then the early greening would be less marked than presented here and may not occur in all ecosystems.

## ACKNOWLEDGMENTS

We thank Tim Kittel and the VEMAP data group at NCAR (Boulder, Colorado) for providing us with the climate scenarios, and David Yates from the Research Application Program, NCAR (Boulder, Colorado), for providing us with PDSI data. We also thank Steve Wondzell, Andy Hansen, Virginia Dale, and two anonymous reviewers for helpful comments on the manuscript. This work was funded in part by the US Department of Energy, National Institute for Global Environmental Change, Great Plains Region (LWT 62-123-06509); the US Geological Survey, Biological Resources Division, Global Change Program (CA-1268-1-9014-10); and the USDA Forest Service, PNW, NE, SE Stations (PNW 95-0730).

## REFERENCES

- Birdsey RA, Heath LS. 1995. Carbon changes in U.S. forests. In: Joyce A, editor. Productivity of America's forest and climate change. General technical report RM-271 Fort Collins, (CO): USDA Forest Service, Rocky Mountain Forest and Range Experiment Station, p 56–70.
- Brovkin V, Ganopolski A, Svirezhev Y. 1997. A continuous climate–vegetation classification for use in climate–biosphere studies. *Ecol Model* 101:251–61.
- Changnon SA. 1989. The 1988 drought, barges, and diversion. *Bull Am Meteorol Soc* 70:1092–104.
- Ciais P, Tans PP, Trolier M, White JWC, Francey RJ. 1995. A large northern hemisphere terrestrial CO<sub>2</sub> sink indicated by the <sup>13</sup>C/<sup>12</sup>C ratio of atmospheric CO<sub>2</sub>. *Science* 269:1098–102.
- Cramer W, Bondeau A, Woodward FI, Prentice IC, Betts R, Brovkin V, Cox PM, Fischer V, Foley JA, Friend AD, and others. 2001. Global responses of terrestrial ecosystem structure and function to CO<sub>2</sub> and climate change: results from six dynamic global vegetation models. *Global Change Biol*. Forthcoming.

- Cramer W, Kicklighter DW, Bondeau A, Moore IIIB, Churkina G, Nemry B, Ruimy A, Schloss AL, and the participants of the Potsdam NPP model intercomparison. 1999. Comparing global models of terrestrial net primary productivity (NPP): overview and key results. *Global Change Biol* 5 Suppl 1:1–15.
- Cubasch U, Cess RD. 1990. Processes and modeling. In: Houghton HT, Jenkins GJ, Ephraums JJ editors. *Climate change: the IPCC scientific assessment*. Cambridge (UK): Cambridge University Press, p 69–91.
- Daly C, Bachelet D, Lenihan JM, Neilson RP, Parton W, Ojima D. 2000. Dynamic simulation of tree–grass interactions for global change studies. *Ecol Appl* 10(2):449–69.
- Diaz HF. 1983. Some aspects of major dry and wet periods in the contiguous United States, 1895–1981. *J Climate Appl Meteorol* 22:3–16.
- Eamus D. 1991. The interaction of rising CO<sub>2</sub> and temperatures with water use efficiency. *Plant Cell Environ* 14:843–52.
- Fan S, Gloor M, Mahlman J, Pacala S, Sarmiento JL, Takahashi T, Tans P. 1998. Atmospheric and oceanic CO<sub>2</sub> data and model simply a large terrestrial carbon sink in North America. *Science* 282:442–46.
- Foley JA, Prentice IC, Ramankutty N, Levis S, Pollard D, Sitch S, Haxeltine A. 1996. An integrated biosphere model of land surface processes, terrestrial carbon balance, and vegetation dynamics. *Global Biogeochem Cycles* 10:603–28.
- Fung I, Field CB, Berry JA, Thompson MV, Randerson JT, Malmstrom CM, Vitousek PM, Collatz GJ, Sellers PJ, Randall DA, and others. 1997. Carbon 13 exchanges between the atmosphere and biosphere. *Global Biogeochem Cycles* 11:507–33.
- Gates WL, Henderson-Sellers A, Boer GJ, Folland CK, Kitoh A, McAvaney BJ, Semazzi F, Smith N, Weaver AJ, Zeng Q-C. 1996. Climate models—evaluation. In: Houghton JT, Meira Filho LG, Callander BA, Harris N, Kattenberg A, Maskell K, editors. *Climate change 1995: the science of climate change. Contribution of Working Group I to the Second Assessment Report of the Intergovernmental Panel of Climate Change*. Cambridge (UK): Cambridge University Press. p 235–84.
- Houghton RA, Hackler JL, Lawrence KT. 1999. The U.S. carbon budget: contributions from land-use change. *Science* 285:574–78.
- Karl TR. 1998. Regional trends and variations of temperature and precipitation. In: Watson RT, Zinyowera MC, Moss RH, Dokken DJ, editors. *The regional impacts of climate change: an assessment of vulnerability*. Cambridge (UK): Cambridge University Press. p 412–25.
- Kattenberg A, Giorgi F, Grassl H, Meehl GA, Mitchell JFB, Stouffer RJ, Tokioka T, Weaver AJ, Wigley TML. 1996. Climate models—projections of future climate. In: Houghton JT, Meira Filho LG, Callander BA, Harris N, Kattenberg A, Maskell K, editors. *Climate change 1995: the science of climate change. Contribution of Working Group I to the Second Assessment Report of the Intergovernmental Panel on Climate Change*. Cambridge (UK): Cambridge University Press. p 285–357.
- Kittel TGF, Rosenbloom NA, Painter TH, Schimel DS, VEMAP Modeling Participants. 1995. The VEMAP integrated database for modeling United States ecosystem/vegetation sensitivity to climate change. *J Biogeog* 22:857–62.
- Küchler AW. 1975. Potential natural vegetation of the United States. 2nd ed. Map 1:3,168,000. New York: American Geographic Society.
- Leenhouts B. 1998. Assessment of biomass burning in the conterminous United States. *Conserv Ecol* 2(1):1. [online]
- Lenihan JM, Daly C, Bachelet D, Neilson RP. 1998. Simulating broad-scale fire severity in a dynamic global vegetation model. *Northwest Sci* 72:91–103.
- Linacre ET. 1977. A simple formula for estimating evaporation rates in various climates, using temperature data alone. *Agric Meteorol* 18:409–24.
- Marks D, Kimball J, Tingey D, Link T. 1998. The sensitivity of snowmelt processes to climate conditions and forest cover during rain-on-snow: a case study of the 1996 Pacific Northwest flood. *Hydrol Proc* 12:1569–87.
- Mckenney MS, Rosenberg NJ. 1993. Sensitivity of some potential evapotranspiration estimation methods to climate change. *Agric For Meteorol* 64:81–110.
- Neilson RP. 1986. High-resolution climatic analysis and southwest biogeography. *Science* 232:27–34.
- Neilson RP. 1995. A model for predicting continental scale vegetation distribution and water balance. *Ecol Appl* 5(2):362–85.
- Neilson RP, Drapek RJ. 1998. Potentially complex biosphere responses to transient global warming. *Global Change Biol* 4:505–21.
- Neilson RP, Marks D. 1994. A global perspective of regional vegetation and hydrologic sensitivities from climatic change. *J Veget Sci* 5:715–30.
- Neilson RP, Prentice IC, Smith B, Kittel TGF, Viner D. 1998. Simulated changes in vegetation distribution under global warming. In: Watson RT, Zinyowera MC, Moss RH, Dokken DJ, editors. *The regional impacts of climate change: an assessment of vulnerability*. Cambridge (UK): Cambridge University Press. p 439–56.
- Nicholls N, Gruza GV, Jouzel J, Karl TR, Ogallo LA, Parker DE. 1996. In: Houghton JT, Meira Filho LG, Callander BA, Harris N, Kattenberg A, Maskell K, editors. *Climate change 1995: the science of climate change. Contribution of Working Group I to the Second Assessment Report of the Intergovernmental Panel of Climate Change*. Cambridge (UK): Cambridge University Press. p 133–192.
- Nigam S, Barlow M, Berbery EH. 1999. Analysis links Pacific decadal variability to drought and streamflow in the United States. *EOS* 80:621–5.
- Palmer WC. 1965. Meteorological drought. Research paper no. 45. Washington (DC): US Weather Bureau, 58 p.
- Parton WJ, Schimel DS, Cole CV, Ojima D. 1987. Analysis of factors controlling soil organic levels of grasslands in the Great Plains. *Soil Sci Soc Am* 51:1173–9.
- Sampson NR. 1997. Forest management, wildfire and climate change policy issues in the 11 western states. CR-820-797-01-0. p 1–44 (<http://www.amfor.org>)
- Schimel DS. 1995. Terrestrial ecosystems and the global carbon cycle. *Global Change Biol* 1:77–91.
- Schimel DS, Melillo J, Tian H, McGuire AD, Kicklighter D, Kittel TGF, Rosenbloom N, Running S, Thornton P, Ojima D, and others. 2000. The contribution of increasing CO<sub>2</sub> and climate to carbon storage by natural and agricultural ecosystems of the US 1980–1993. *Science* 287:2004–6.
- Scurlock JMO, Cramer W, Olson RJ, Parton WJ, Prince SD. 1999. Terrestrial NPP: toward a consistent data set for global model evaluation. *Ecol Appl* 9:913–9.

Sitch S. 2000. The role of vegetation dynamics in the control of atmospheric CO<sub>2</sub> content [dissertation]. Lund University (Sweden): Institute of Ecology.

[VEMAP] Members. Vegetation/Ecosystem Modeling and Analysis Project. 1995. Vegetation/ecosystem modeling and analysis project: comparing biogeography and biogeochemistry

models in a continental-scale study of terrestrial ecosystem responses to climate change and CO<sub>2</sub> doubling. *Global Biogeochem Cycles* 9:407–37

Woodward FI, Lomas MR, Betts RA. 1998. Vegetation–climate feedbacks in a greenhouse world. *Philos Trans R Soc London B* 353:29–38.